European Journal of Pharmaceutics and Biopharmaceutics 76 (2010) 311–319

Contents lists available at ScienceDirect

European Journal of Pharmaceutics and Biopharmaceutics

journal homepage: www.elsevier.com/locate/ejpb

Research paper

Relationships between solid dispersion preparation process, particle size and drug release – An NMR and NMR microimaging study

Carina Dahlberg [a,b], Anna Millqvist-Fureby [b], Michael Schuleit [c], István Furó [a,*]

[a] Department of Chemistry, Royal Institute of Technology, Stockholm, Sweden
[b] YKI, Institute for Surface Chemistry, Stockholm, Sweden
[c] Novartis Pharma AG, Pharmaceutical and Analytical Development, Basel, Switzerland

ARTICLE INFO

Article history:
Received 1 December 2009
Accepted in revised form 10 June 2010
Available online 16 June 2010

Keywords:
Gel layer formation
Rotoevaporation
Spray drying
Hydroxypropyl methylcellulose
HPMC
Diffusion

ABSTRACT

Solid dispersion tablets prepared by either spray drying or rotoevaporation and exhibiting different grain and pore sizes were investigated under the process of hydration-swelling-gelation. ^{2}H and ^{1}H NMR microimaging experiments were used to selectively follow water penetration and polymer mobilization kinetics, respectively, while the drug release kinetics was followed by ^{1}H NMR spectroscopy. The obtained data, in combination with morphological information by scanning electron microscopy (SEM), reveal a complex process that ultimately leads to release of the drug into the aqueous phase. We find that the rate of water ingress has no direct influence on release kinetics, which also renders air in the tablets a secondary factor. On the other hand, drug release is directly correlated with the polymer mobilization kinetics. Water diffusion into the originally dry polymer grains determines the rate of grain swelling and the hydration within the grains varies strongly with grain size. We propose that this sets the stage for creating homogeneous gels for small grain sizes and heterogeneous gels for large grain sizes. Fast diffusion through water-rich sections of the inhomogeneous gels that exhibit a large mesh size is the factor which yields a faster drug release from tablets prepared by rotoevaporation.

1. Introduction

Formulating solid dosage forms with specific dissolution profiles is of fundamental importance for the pharmaceutical industry. The dissolution process is affected in a complex way by many factors such as the physical state of the drug, the nature of the excipient or the tablet coating and the porosity. Hence, it is, in general, difficult to predict the dissolution behaviour of solid matrices. This is particularly the case when considering tablets made of solid dispersions.

Solid dispersions, which can facilitate oral delivery of drugs with poor water solubility, consist of a hydrophilic polymer matrix in which the drug is finely dispersed [1]. The drug can be in the state of small crystalline or amorphous particles and, in the ultimate limit, the dispersion is on the molecular level. Distinguishing between these physical states is far from trivial. Irrespective of the dispersion level, the tablet dissolution and the release of drug substances can be described schematically as a multistep process, including wetting, water uptake and transport, loosening of the polymer matrix and the subsequent dissolution and transport of drug. The transport processes involved are assumed to be affected by the change they themselves cause, since the initially solid polymer matrix gradually transforms into a gel with a continuously disintegrating edge toward the water phase [2]. The general perception is that this gel layer acts as a transport barrier. The barrier performance is governed by many factors including the molecular size of the drug, local concentrations, molecular and particle size of the polymer, and even air entrapped in the tablets [3,4].

Solid dispersions may be manufactured by different processes, such as melting or solvent methods [1,5]. One of the areas that has not received much attention is the relevance of the manufacturing technique and the resulting particle size for the physical properties such as swelling and release kinetics. Related investigations into *physical mixtures* indicated that the effect of polymer particle size on drug release is dependent on the polymer concentration [3,6–9]. In mixtures with polymer concentration in the range of the ones used in this study (85 w%, see below), the effect of polymer particle size on drug release was negligible. The explanation presented was that, at high polymer concentrations, the formed gel layers are homogeneous irrespective of the polymer particle size and thereby retard the drug to an equal extent. In physical mixtures with low polymer concentrations, a trend of increasing drug release rate with increased particle size was observed [2–4,6–10]. This effect was explained by assuming that particles of increasing size require increasing time for water

* Corresponding author. Address: Division of Physical Chemistry and Industrial NMR Centre, Department of Chemistry, Royal Institute of Technology, SE-100 44 Stockholm, Sweden. Tel.: +46 8 7908592; fax: +46 8 7908207.
E-mail address: ifuro@physchem.kth.se (I. Furó).

0939-6411/$ - see front matter © 2010 Published by Elsevier B.V.
doi:10.1016/j.ejpb.2010.06.006

penetration, which delays the formation of a homogeneous gel barrier. The contribution of air trapped within the pores adds some controversy with studies reporting either significant [11,12] or negligible [13] effect on drug dissolution and release. However, none of the results obtained in physical mixtures can be transferred directly to solid dispersions, where the drug is incorporated in the polymer matrix rather than distributed between the polymer particles as in physical mixtures.

It should be pointed out that comparing drug release obtained in various pharmaceutically relevant solid dispersions is not straightforward, since a large variation can result from the spread of the physical and chemical properties of the incorporated poorly water-soluble drug. To overcome this problem, model systems are useful. The model system used in this work, containing a rather soluble drug, allows us to link differences in release data to bulk structural properties of the tablets.

Experimental techniques are often insufficient to characterize both structural effects, molecular state and transport during tablet swelling. As an example, conventional dissolution tests give information about the amount of drug and polymer in the liquid phase, but not about the molecular and structural features in the tablet. Scanning electron microscopy (SEM), while popular and capable as concerning structural details, is limited to dry tablets. Here, we explore nuclear magnetic resonance (NMR) spectroscopy and NMR imaging as tools for measuring water penetration, polymer swelling and drug release in parallel and in a non-invasive manner. The versatility of NMR makes it particularly suitable to probe this multifaceted phenomenon [14,15]. As demonstrated below, the ability and the sensitivity of NMR spectroscopy and NMR imaging to monitor molecular dynamics in complex polymer matrices points to the potential of these methods in drug delivery systems. In earlier NMR-based studies, the focus has been on solvent diffusion into the matrix during swelling [16–22]. In this work, the goal is to elucidate the impact of tablet structure on polymer swelling and drug release in solid dispersions.

2. Materials and methods

2.1. Chemicals

Antipyrine (Sigma–Aldrich) was used as a model drug. Since it is has a rather high solubility in water, its aqueous concentration can be easily recorded by NMR. Commercially available hydroxypropyl methylcellulose, HPMC, (Dow Chemical, USA) was used as carrier material. Ethanol (Alco Suisse), acetone (Shell) and distilled water were used in preparation of the solid dispersions. Deuterated water, D_2O, (99.9 atom% D, Sigma–Aldrich) was used as penetrant liquid for all the experiments, except for the qualitative ^1H NMR imaging experiments of water where degassed distilled water was used.

2.2. Sample preparation

First, the antipyrine was dissolved in a mixture of ethanol, acetone and water at 40:40:20 w%. Subsequently, the polymer (HPMC) was dispersed in this solution and was allowed to swell and dissolve for at least 1 h. The resulting solutions had a solvent/polymer ratio of 10:1 and a drug concentration of 15 w%, relative to polymer weight.

The solvents were subsequently evaporated from the obtained solutions by two different methods which differ by the rate at which the solvent is removed, and the final structure of the dry solid dispersions. Rotoevaporation (RO) was carried out in a rotary evaporator (Rotavapor R-200/205, Büchi, Switzerland) under reduced pressure at about 40 °C until a dry material was obtained. This material was then milled in a small agate ball mill and passed through either a 60 μm or a 200-μm mesh (DIN-4188) to obtain powders with two particle size distributions (<60 μm and <200 μm, respectively). The tablets prepared from these powders will be referred to as RO-60 and RO-200, respectively.

In spray drying (SD), the solutions were dispersed in a spray dryer (Büchi Mini Spray Dryer B-290, Büchi Switzerland) with a two-fluid nozzle (Schlick Modell 0/2) and dried by a nitrogen gas stream. The inlet air temperature was 140 °C, and the outlet temperature was kept at 60 °C. Liquid feed was 12 mL/min, and the drying airflow was 0.3 m^3/min. The obtained particles/granules were separated by a cyclone. The diameter of the particles ranged from 2 μm to 20 μm with an approximate average particle diameter of 10 μm, determined by visual inspection of scanning electron microscopy (SEM) images. The tablets prepared from these powders will be referred to as SD-10.

All powders were stored at 8 °C in a closed container. Portions of powders, corresponding to the intended tablet weights (129 ± 1 mg for the 2D imaging experiments and 97 ± 1 mg powder for the other experiments), were directly compressed with cylindrical flat-faced punches (8 mm in diameter) and die using a laboratory press (Specac, England). The approximate tablet density was 0.92 ± 0.02 g/cm^3 (where the primary source of scatter arises partly from the uncertainty in estimating the tablet height and partly from any irreproducibility of the height). Considering the approximately 1.3 g/cm^3 density of HPMC, this indicates a roughly 30% porosity of the tablets. The different weights had no impact on the water penetration and swelling behaviour onward from the exposed tablet edge (demonstrated by separate experiments, not shown).

The flat-faced tablets were inserted at the bottom of a Teflon tube (with an inner diameter of 8 mm), so that the tablet swelling and the drug release were restricted to one dimension. Layering 4 ml D_2O on the tablet top initiated swelling (time = 0). The tube was then quickly inserted into the NMR magnet, and the experiments were commenced. For trials with air evacuation, the tablet in the tube was first subjected to vacuum (1–2 mbar for 20 min) before the water was allowed to break the vacuum. The water layered on the tablet top prevented re-entry of air into the tablet. Experiments with evacuated tablets will be referred to as ROvac-200 and SDvac-10, respectively. We note that the liquid volume used (4 ml) was sufficient to allow drug release and tablet swelling to proceed without significant limitations due to the solubility of the drug (the solubility of antipyrine is 6.8 mg/mL, and 14.6 mg was contained in the ca 2 mm high thinner tablet of 97 ± 1 mg weight on which the quantitative experiments were performed). This is particularly true for the initial behaviour (see Fig. 2 below). When comparing our results to those of other experiments, the reader is reminded that we have no sink condition in the external medium and no stirring.

2.3. Experiments

2.3.1. ^1H and ^2H NMR Imaging

All imaging experiments were performed on a Bruker Avance II 300 spectrometer equipped with a Bruker GREAT-60 gradient unit and a Bruker microimaging probe (Micro 2.5).

Qualitative two-dimensional (2D) ^1H NMR imaging of water distribution was performed using a fast low angle shot imaging pulse sequence, FLASH [23], with a repetition time of 101.5 ms, an echo time of 3.3 ms and 8 scans. The field-of-view was 8.5 mm in any direction and with an acquisition matrix size of 128 × 128 this provided a resolution of 67 μm. Vertical slices, parallel to the tablet axis, and horizontal slices at different heights within the tablets were acquired, all with a slice thickness of 0.5 mm, at different times during the water penetration process.

Below, we present the horizontal slice at the upper gel phase and the vertical slice through the tablet axis. A short recycling delay is demanded in order to acquire images reasonably fast, with respect to the time scale of the water penetration process. This latter choice significantly reduced the signal from water with high mobility and rendered our 2D images, while clearly illustrative of structural features, not quantitative. The acquisition time for a 2D image was approximately 2 min.

One-dimensional (1D) vertical profiles illustrating either the quantitative distribution of water or the mobility of the HPMC polymers during the swelling process, were acquired, respectively, by conventional ^{2}H spin-echo imaging based on Hahn's spin-echo pulse sequence [26] (for water) or by 1D ^{1}H constant time imaging (CTI) [24,25] (for HPMC profiles). Relative advantages and disadvantages of this strategy were discussed in [27].

The CTI technique was used since it provides high-quality images even for solid or semi-solid materials. We stress that, with heavy water as penetrant liquid, ^{1}H profiles dominantly arise from the non-exchangeable protons of the polymer component with minor possible contribution from the dissolving drug and protons transferred to the penetrating water (see detailed discussion in [27]). On the other hand, the ^{2}H profiles arise dominantly from water (even if proton exchange is fast ^{1}H remains very dilute in the added 4 ml of D_2O). The ^{1}H CTI experiments were performed with a phase encoding time of 79 μs, a flip angle of 15° (pulse length 2.5 μs) and a gradient strength of 147.5 G/cm. Using 32 scans, the time for acquiring one profile was 7 min. With a field-of-view of 12.8 mm, a spatial resolution of 100 μm was obtained. The ^{2}H spin-echo experiments were performed using an rf pulse length of 36 μs for a 90° pulse, a gradient strength of 51 G/cm, a spectral width of 100 kHz, 512 data pixels within a field-of-view of 20 mm, that is, a nominal spatial resolution of 39 μm. With 3 s recycle delay (more than five times longer than the T_1 = 430 ms for ^{2}H measured in pure D_2O), the time resolution of the experiments was 1.5 min. Upon addition of any amount of HPMC, the ^{2}H T_1 value decreases. The echo time was 4 ms, which is short compared to the T_2 > 20 ms for ^{2}H (estimated by slice-selective ^{2}H spin-echo experiments), valid at any water content in HPMC higher than ca 2%. In other words, all our ^{2}H profiles (shown below) remain undistorted by either transverse or longitudinal relaxation effects. Hence, we consider our ^{2}H profiles as quantitative measures of the distribution of the penetrating water. In this context, one should also note that even if proton exchange with the polymer may modify somewhat ^{2}H distribution between polymer and water molecules, any ^{2}H intensity detected for a region within the tablet volume must arise from water molecules that have penetrated into the region in question.

We stress that, as previously discussed [27], if water profiles had been measured by ^{1}H NMR and H_2O as penetrant liquid, 1D profiles could not have been quantitatively representative of the water content because of both proton exchange and the appearance of the mobile polymer component upon swelling.

2.3.2. ^{1}H NMR Spectroscopy

The release experiments were performed on a Bruker DRX500 spectrometer, operating at a ^{1}H frequency of 500 MHz and equipped with a Bruker microimaging probe (Micro 5). The sample was placed below the lower border of the sensitive region of the radiofrequency (rf) coil of the probe in order to eliminate the signal from the tablet and the gel layer [27]. Conventional spectra were acquired by averaging 16 scans using a single 90° rf pulse. Collecting one spectrum took 4 min. A thin capillary with tetramethylsilane (TMS) was used as a quantitative reference as well as a chemical shift reference. The setup was carefully tested to ensure reproducibility. Experiments were performed every fourth minute (the initial 9 h are shown here), and the (relative) antipyrine concentration was established by spectral integration. The outer fringes of a 2.9 ppm wide spectral section with the two representative antipyrine peaks at its centre and a 2.6 ppm wide spectral section with the reference TMS peak at its centre were subjected to minor manual baseline correction. Integration was performed in 0.9 ppm and 1 ppm wide spectral windows for antipyrine and TMS, respectively. All measurements were repeated four times, and the average value is reported.

2.3.3. Scanning electron microscopy (SEM)

An XL30 ESEM (Philips) scanning electron microscope was employed in high vacuum mode for characterization of the powder structure. Before analysis, the samples were gold coated (180 s, 40 mA) using a Balzers SCD050 coater. SEM images were obtained using a mix of backscatter and secondary electron detectors.

3. Results

In this study, we have focused on the effects of structural properties on gel layer formation, water penetration and polymer mobilization during tablet dissolution in order to find a relationship between the release rate and the structural properties and particle size distribution caused by the preparation technique. An additional potential question was the possible effect of entrapped air.

Experiments have been performed on three types of tablets prepared, respectively, from three types of powders; SD-10 having an average particle size of 10 μm prepared by spray drying, RO-200 (particle sizes <200 μm) and RO-60 (particle sizes <60 μm) prepared by rotoevaporation in combination with milling and sieving. In order to investigate whether air entrapped during tabletting affects the gel layer formation and the drug release, the behaviour of SD-10 and RO-200 tablets was also studied by experiments involving an evacuation step (ROvac-200 and SDvac-10, see above).

3.1. Chemical and structural properties

The morphological differences between the powders and tablets were analysed by scanning electron microscopy (SEM). The solid dispersions prepared by RO exhibit large and compact particles with irregular forms and sharp edges as a result of milling. Mainly round particles with wrinkled surfaces are observed for the SD powders. Both the difference in grain character and the difference in the size and number of pores in the compressed tablets are illustrated in Fig. 1.

The chemical composition at the surface and the contact angle of water on the compressed tablets have been analysed by X-ray photoelectron spectroscopy (XPS) and dynamic absorption tester (DAT) analysis, respectively, as described previously [28]. All tablet surfaces were shown to have approximately the same drug coverage (2–4%) and contact angles (57–58°). In addition, the average concentrations of antipyrine in the bulk of the different powders were shown to be approximately the same (within the experimental error) by UV–Vis-spectroscopy.

All prepared solid dispersion powders were shown to lack crystalline drug particles of significant size and amount, as has been verified by the lack of accompanying features in differential scanning calorimetry (DSC) scans and in powder X-ray diffraction (pXRD) patterns. This has been tested for powders directly after preparation, after six month in dry storage and after an additional six weeks at 30% relative humidity. pXRD experiments on compressed tablets also confirmed that tablet compression did not induce recrystallization of the drug.

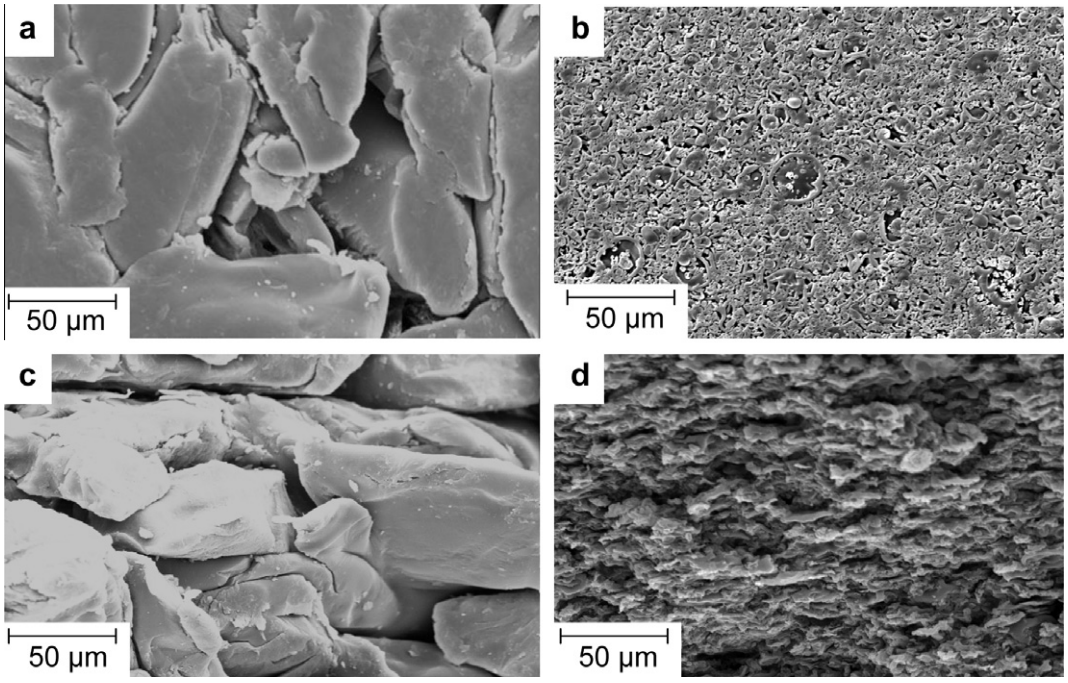

Fig. 1. SEM images of an RO-200 tablet (a) and (c) and an SD-10 tablet (b) and (d); (a) and (b) are upper surfaces (to be in contact with water) while (c) and (d) are breakage surfaces.

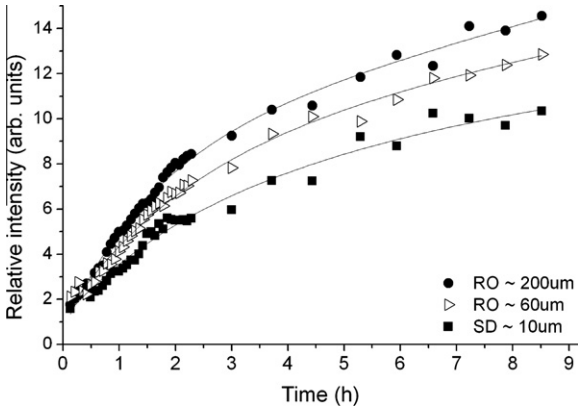

Fig. 2. Comparison of the amount of drug (antipyrine) released from RO-200 (●), RO-60 (▷) and SD-10 tablets (■) into the aqueous phase. The amount released after 9 h is approximately 10% of the total drug contained in the tablet. The lines are a guide for the eye. The maximum estimated intensity error was ± 5%, relative to the highest intensity presented here.

3.2. Release of model drug substance

The relative amounts of released antipyrine from RO-200, RO-60 and SD-10 tablets during swelling, as measured by ^{1}H NMR spectroscopy in the aqueous phase above the tablet, are shown for the initial 9 h in Fig. 2. A clear trend of faster release for larger particle size is seen through the whole tablet dissolution process (which takes several days under static conditions). All experiments have been performed four times with good reproducibility (maximum estimated relative intensity error was ±5%). The trend holds even if quantitative results from different sample batches may slightly differ. It should be stressed that by using model systems, incorporating a rather simple water-soluble drug, the obtained differences in release originate from the variation in tablet structure.

All release curves exhibit a time dependence similar to that previously established [27]. One should also note that the release curves in Fig. 2 exhibit the same functional form of time dependence; in other words, the different curves are well scalable on each other by constant factors (for example, by scaling 1:1.18:1.42 for the specific data shown in Fig. 2). Evacuating the air from the tablets had no significant effect on the drug release (release curves not shown).

3.3. Imaging of gel layer formation

By acquiring ^{1}H NMR images of the tablets at different times after hydration, the gel formation processes could be followed in detail. Some differences are well illustrated by horizontal and vertical slices through the tablets, see examples of the former in Fig. 3. To keep the time required for recording an image short, the quantitative nature of the images has been sacrificed (see Section 2.3.1).

To interpret the images, one must recall that they were recorded by relatively long echo times (3.3 ms). Hence, image

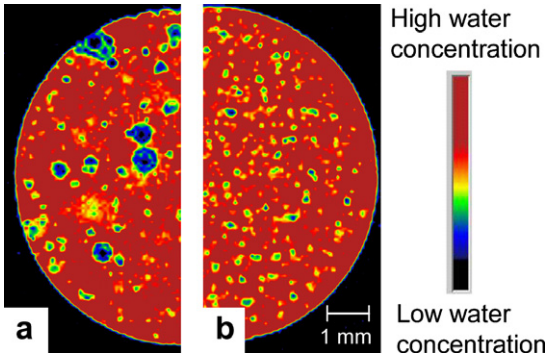

Fig. 3. Horizontal ^{1}H NMR image slices of an RO-200 (a) and an SD-10 (b) tablet recorded 2 h after the onset of tablet hydration. The colours provide a qualitative representation of the water concentration in the samples (see colour bar). The slice has been positioned at the height of surface of the originally dry tablet. (For interpretation of the references to colour in this figure legend, the reader is referred to the web version of this article.).

intensity is dominated by water molecules while signal contribution from rigid polymers, yet to be mobilized by water, is negligible. Hence, dark areas in the images indicate lack of water. By two arguments, most dark areas displayed either in Fig. 3 or in Fig. 4 can be assigned to air-filled voids. First, most dark spots are larger, sometimes much larger, than the upper limit of particles size for the powders used. Hence, dry single polymer grains cannot cause the observed appearance of the images. However, blocked pore pathways could still be imagined to create poorly hydrated regions. However, this explanation can be excluded by observing the movements of dark spots during tablet swelling. Fig. 4 shows one horizontal slice and four vertical slices recorded at different times through a RO-200 tablet. Dark spots labelled 1–3 move clearly upward and ahead of the swelling front. Since the specific gravity of HPMC is higher than that of water [29] this excludes those regions being poorly hydrated polymer grains. In previous studies where swelling of hydrophilic matrixes has been characterized [11,13,30,31], it has been assumed or stipulated that voids primarily appear because of air entrapped in the original pores. That could, by assuming coalescence of bubbles enabled by the formation of a soft gel, also explain why the dark spots are larger than the voids observable in the SEM images. In this context we note that, in contrast to previous experiments where dark spots disappeared from some images recorded after having the air evacuated [31], the reduction in the number and size of dark spots was, if any, moderate in our experiments performed with air evacuation. Hence, we conclude that voids form, but cannot confirm that it is entrapped air only that prevents water from reaching some parts of the tablet; blocking of pores by the evolving gel might also be a factor. If so, large external field gradients produced by the magnetic susceptibility differences at the void/gel interface [32] can be invoked as an additional factor that determines the apparent size of the observed dark spots.

The 1D water penetration profiles obtained by ^{2}H NMR imaging and shown in Figs. 5 and 6 provide a quantitative characterization of water penetration. Since no other molecular component contains a significant amount of the ^{2}H isotope, the maximum signal intensity is defined as 100% water content, and a lower intensity represents a proportionally lower water content. By comparing the water concentrations at different positions in the originally dry tablet, a slightly faster water penetration in the SD-10 tablets compared to that in the RO-200 tablets is observed. Air evacuation accelerated water penetration into RO-200 tablets and, to a smaller extent, into SD-10 tablets (Fig. 6) and even reversed the relative order of the two tablets as concerning water penetration rate.

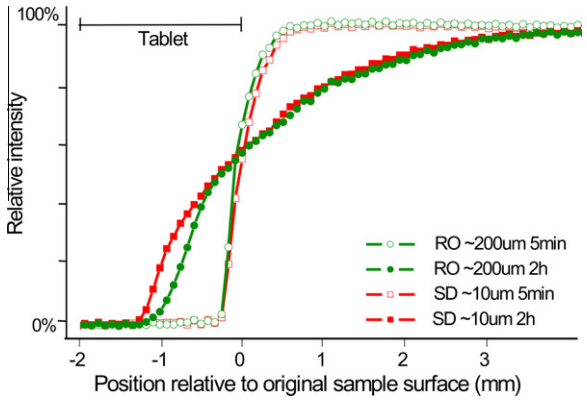

Fig. 5. One-dimensional vertical water profiles recorded by ^{2}H NMR imaging in RO-200 tablets and SD-10 tablets, both of 2 mm dry height, at times 5 min and 2 h after the onset of tablet hydration. See Fig. 6 for profiles acquired at intermediate times.

A selection of 1D polymer mobilization profiles obtained by ^{1}H constant time imaging (CTI) is shown in Figs. 7 and 8. Hydration of the polymers increases their transverse relaxation time, which leads to higher image intensity [24,27]. Hence, within the volume of the originally dry tablet intensity change reflects a change in molecular mobility. Outside that volume and in the outwardly expanding gel layer, an increase in intensity represents a combination of increased mobility and an increased amount of polymers (recall that, with heavy water added, the signal contribution from water is small). We stress that the polymer mobilization profiles in Figs. 7 and 8 are not quantitative and, while having the same horizontal axis, cannot be directly compared to the water concentration profiles in Figs. 5 and 6.

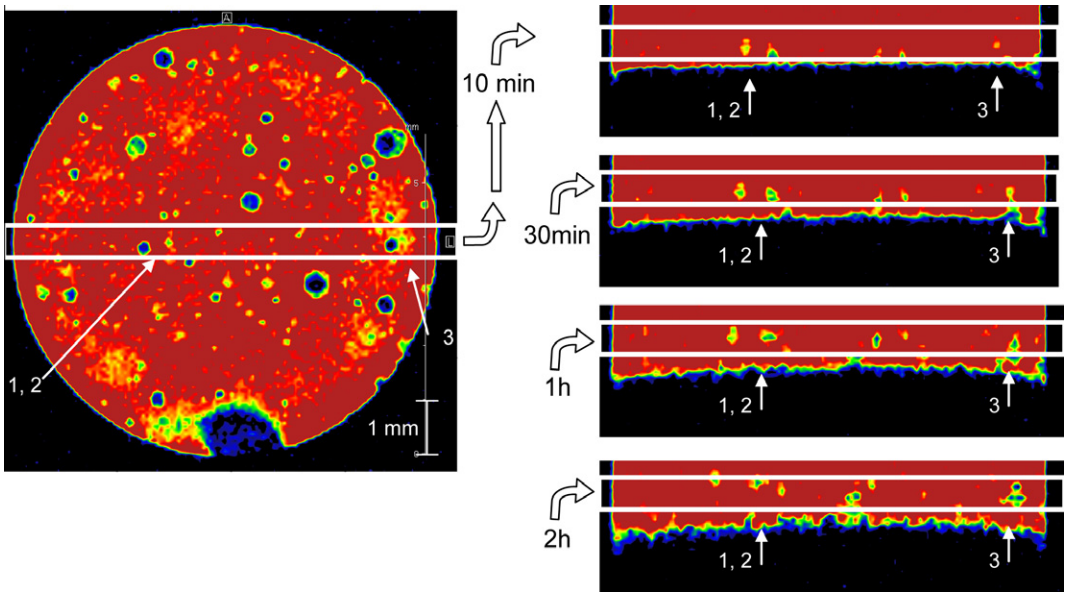

Fig. 4. One horizontal and four vertical ^{1}H NMR image slices (with slice width of 0.5 mm) of an RO-200 tablet. Bubbles labelled 1, 2 and 3 can be followed on their way through the gel layer. The white rectangle in the horizontal image indicates the position of the recorded vertical slices and *vice versa*. The spatial scale bar given in the horizontal cross-section image is valid for all images. The horizontal slice has been positioned at the height of surface of the originally dry tablet. (For interpretation of the references to colour in this figure legend, the reader is referred to the web version of this article.).

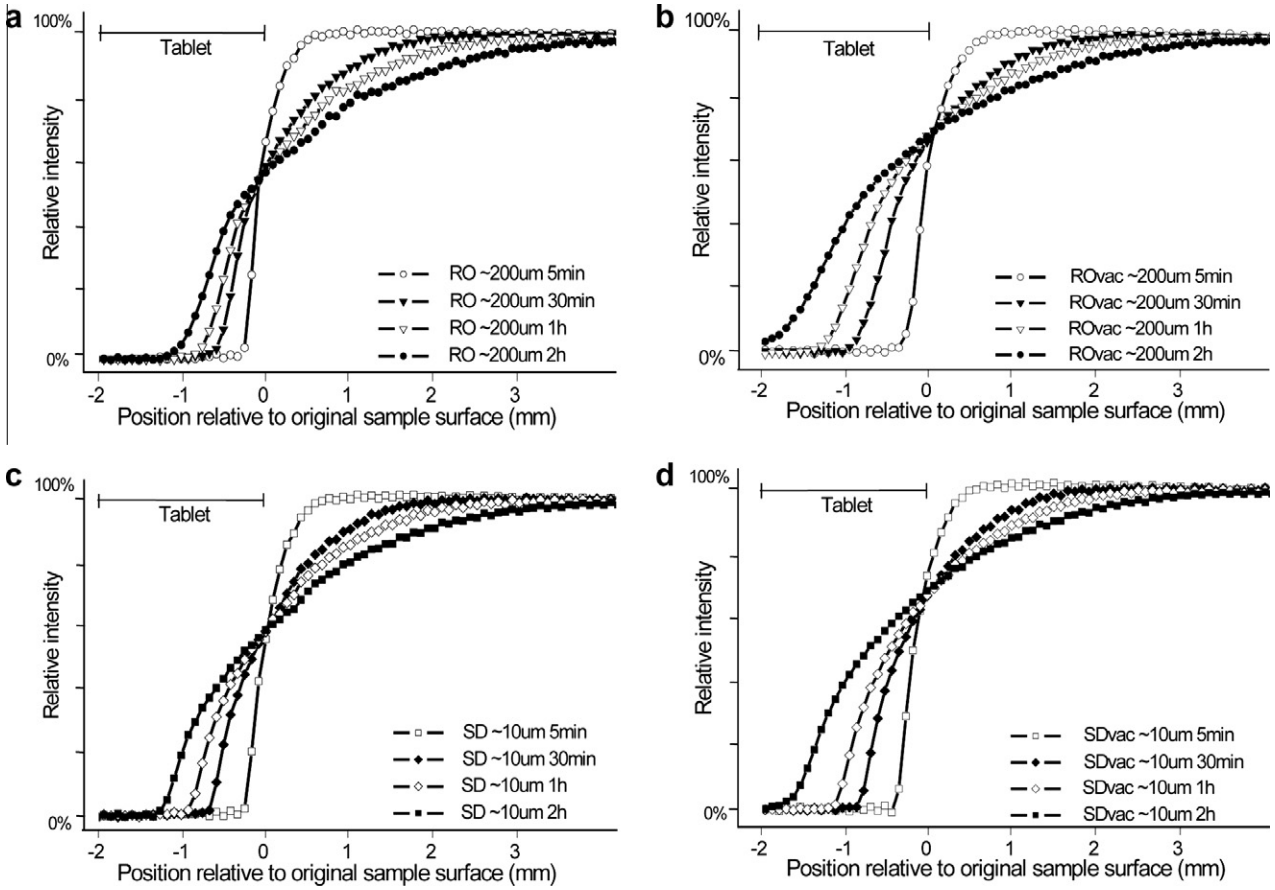

Fig. 6. One-dimensional vertical water profiles recorded by ^{2}H NMR imaging in RO-200 tablets and SD-10 tablets, all of 2 mm dry height, at different times after the onset of tablet hydration. Data for tablets hydrated without (a/c) and with air evacuation (b/d) are shown.

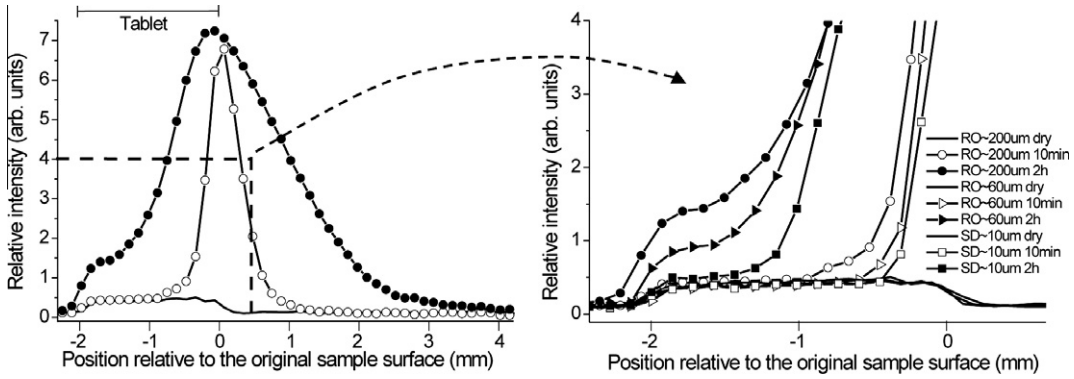

Fig. 7. One-dimensional vertical polymer mobility profiles recorded by ^{1}H NMR imaging for RO-200, RO-60 and SD-10 tablets, all of 2 mm dry height, at times 5 min and 2 h after the onset of tablet hydration. See Fig. 8 for profiles acquired at intermediate times. Non-zero image intensities below the lower tablet edge (−2 mm) appear because of the finite spatial resolution of 100 μm.

Fig. 7 shows that a larger grain size resulted in a faster spread of the hydrated and mobilized polymer front. Additionally, the penetration of this latter front is homogeneous for the SD-10 tablets as indicated by the signal level toward the bottom end of the tablet (see Fig. 8c). The low constant signal level, similar to the one of the dry material, indicates that no part of the lower regions is hydrated until reached by a uniformly spreading hydration front. In contrast, the bottom of the RO-200 and, to a smaller extent, RO-60 tablets (see Fig. 8a and b) must be reached by some small amount of water since the signal level starts to increase before the arrival of the main hydration front. In other words, the hydration of the RO-200 and RO-60 tablets is more heterogeneous than that for the SD-10 tablets. Air evacuation increased the amount of mobilized polymers slightly, but left the kinetics of the polymer mobilization front unchanged. The discussion below will resolve the apparent contradictions that one may perceive when comparing the obtained water and polymer profiles.

4. Discussion

In terms of drug content and wettability, the surfaces of all samples were very similar and these parameters can therefore be

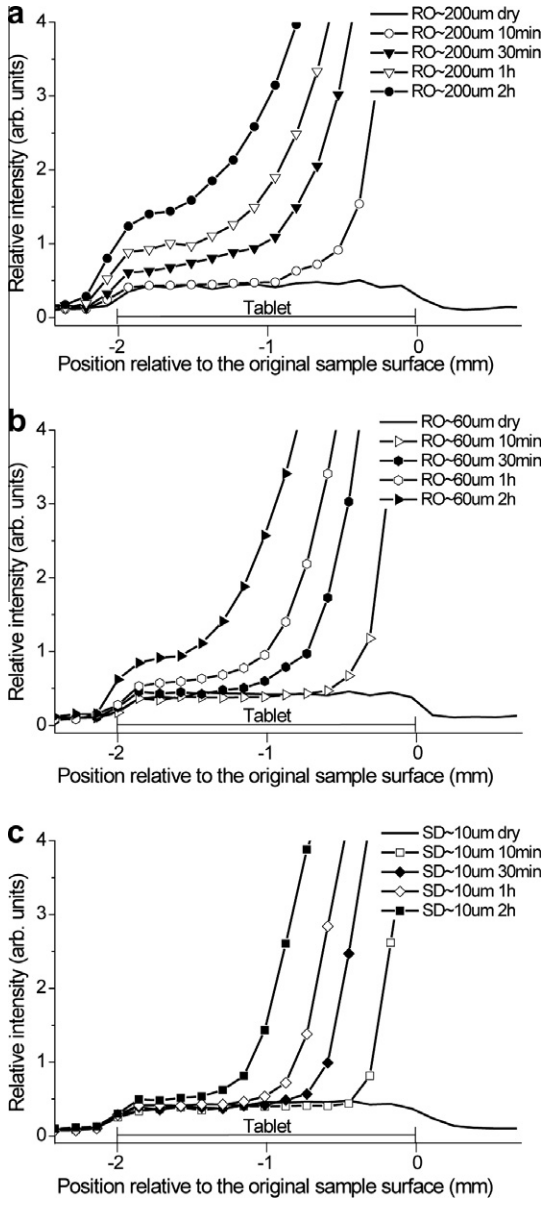

Fig. 8. One-dimensional vertical polymer mobility profiles recorded by ^{1}H NMR imaging for RO-200 (a), RO-60 (b), and SD-10 (c) tablets, all of 2 mm dry height, at different times after the onset of hydration.

excluded as having substantial effects on the gel layer formation and drug release. Furthermore, we have observed that in the rather weak gel that forms above the original tablet surface, both the water and polymer mobilization profiles (at positions more than 0.5 mm above the surface of the originally dry tablet) were very similar for all investigated tablet types. This leads us to the conclusion that the observed difference in drug release must be attributed to the structural properties of the dense gel layer with relatively low water content that forms underneath the original tablet surface during water ingress. The following discussion concerning the morphological effects on gel layer formation, structure and concentration is therefore dedicated to this part of tablet. The weak gel above the original tablet surface will merely delay the drug release by slowing down the diffusion of drug molecules upward, however, that delay will be the same for all tablets involved.

We discount the morphology of the grains and, thereby, the morphology of the porous network that forms when pressing the tablet as important factors. To this claim, we recall that our results obtained on RO-60 tablets were in all means intermediate between the results for the SD-10 and for the RO-200 tablets (see, for example, Fig. 8). Hence, the rougher and sharper edges of particles observed for RO-type tablets and the possibly broader distribution of particle and pore sizes have no distinguishable effect.

We also disregard air in the tablets as a major factor. Undoubtedly, evacuation has an effect on the rate of water penetration as shown in Fig. 6 (with the overlap directly illustrated) and Fig. 5. However, we could not detect changes of comparable magnitude in either drug release or polymer mobilization. Additionally, one should recall that the effect of evacuation on water penetration was much larger for RO-200 than that for SD-10. These observations together suggest that in systems with large pores, and thereby low capillary pressure to aid water ingress, air present in the pores may inhibit water influx. However, both the polymer mobilization and the drug release depend on water uptake by the polymer grains. Hence, our observations indicate that this latter process seems to be the rate-limiting factor rather than getting access to water in nearby pores. At this point, it seems prudent to recall that there exist contradictory results on the effect of air on drug release. On one hand, it has been suggested that the motion of bubbles adds a degree of internal mobility in the tablets, which might result in faster dissolution and release [13]. On the other hand, bubbles and air enclosed in pores were claimed to act as barriers to solute transport [11,33] and to increase the diffusional path length, slowing down the release (at least initially [12]).

Now we recall our most important observation that grain size is correlated with release rate. In addition, the other quantity that is correlated with drug release rate is the polymer mobilization behaviour. We note explicitly, and again, that water penetration rate has no direct effect on drug release as indicated by the lack of effect of evacuation on release rate and the significant simultaneous effect of evacuation on water penetration (see RO-200 data in Fig. 6). Together, these suggest that inhomogeneous gels that form provide a faster release than homogeneous gels. Below, we detail this statement and attempt to formulate a model that is consistent with our observations. When doing so, we elaborate with a concept of solid dispersions where the drug, either molecularly or in particles with size in the order of nanometers, is evenly distributed within the polymer grains. As concerning the complete process of drug release, we shall consider how changes within the tablet may influence the following constituting steps: swelling and fusion of individual polymer grains, gel formation with increasing level of hydration, release of individual drug molecules from the drug particles into the surrounding aqueous gel and, finally, the transport of the drug molecules through the gel into the aqueous supernatant phase.

Consider first the SD-10 tablets where the polymer grains are small. Hence, there is a large surface area that provides good polymer–water contact. Small grains make the pores between the grains small, too (see Fig. 1). Hence, the time required for the hydration of the grain and for a gel to form and block the pores is short. More importantly, hydration is controlled by diffusion of water into the grains, and the time required for the diffusing water to reach the full grain volume does not scale linearly. In the conceptually simplest case with a constant diffusion coefficient [26], for which $\langle x^2 \rangle = 2Dt$, where x is the diffusion pathlength, D is the diffusion coefficient and t is the time, one expects a quadratic dependence with grain size. Any monotonic increase in D with water content leads to an even steeper functional dependence between size and full time for grain hydration. Here, we recall that in SD-10 (i) the polymer mobilization front moves in a homogeneous manner (see Fig. 8c) and (ii) the water penetration front and the mobilized polymer front are closely correlated (compare Figs. 6c and 8c). Hence, water penetration seems not to be controlled by

free and open pores. Instead, pores seem to be quickly blocked by the rapidly hydrating and swelling grains which fuse and create a homogeneous gel layer. In the formed gel, the water is evenly distributed and, because of the homogeneous nature of swelling, the microstructure is also homogeneous resulting in a macromolecular network with an even mesh size.

Concerning the drug component, this scenario has the following consequences. First, since hydration of the polymer grains is a quick process, all drug particles in the penetrated regions are rapidly surrounded by water and can thereby become molecularly dissolved in the formed aqueous gel. Second, to be detected in the experiments that lead to our Fig. 2, the dissolved molecules must diffuse through the gel network. The rate for the diffusive transport depends strongly on the relation between the molecular size of the drug and the polymer mesh size. Concerning this latter point, there exist numerous theoretical models which relate diffusion coefficients of solutes to the mesh size [34,35]. These models predict strongly non-linear, typically exponential-type dependence, of the solute diffusion coefficient on the polymer volume fraction, but the actual numerical factors differ sizeably from model to model. However, there is a wealth of experimental data on diffusion of similarly sized hydrophilic molecules in hydrogels (see references in [34,35]), which provide useful comparisons. The volume density of water at any point can be estimated from our quantitative 1D water images in Fig. 6. Hence, for example, at the surface of the originally dry tablet, the volume density of water is 60–70% of that of liquid water which translates to (under the assumption that air has left the matrix) 30–40% polymer concentration. For an antipyrine-sized molecule, this typically leads to a diffusion coefficient that is approximately one order of magnitude lower (that is, $<10^{-10}$ m^2/s) than that in bulk water. Such a diffusion coefficient sets the time drug molecules need to traverse 1 mm to the order of 10^4–10^5 s. Of course, the mesh size in our tablets varies continuously from a smaller value at the hydration front to an infinitely large value at the point where the gel dissolves. Nevertheless, as illustrated in Fig. 6c and d, 2 h after having initiated tablet swelling, the width of the formed gel layer with >20% polymer content is approximately 2 mm wide. This means that, at this stage in the experiment, diffusive transport of drug molecules from the hydration front to the aqueous phase takes many hours. This explains the finding that after 9 h of swelling only approximately 10% of the drug is released into the aqueous phase (see Fig. 2) although, by that time, the full tablet volume has been accessed by water.

In the RO-200 tablets, two distinctive features when compared to the SD-10 samples are observed: (i) the polymer mobilization front moves in an inhomogeneous manner (see Fig. 8a), and (ii) the water penetration front and the mobilized polymer front are not closely correlated (compare Figs. 6a and 8a). The notion that the advance of the polymer mobilization front is inhomogeneous is based on Fig. 8a: although most of the ingressing water is close to the tablet top, some small amount of water must have reached the very bottom since polymer mobility begins to increase there. We ascribe this to larger pores which enable fast initial water penetration. The same feature also contributes to the other observation, the lack of close correlation between the water penetration front and the mobilized polymer front. Additionally, water penetration into individual grains will be a much slower process than that in SD-10, creating large differences in the level of hydration between grain surface and grain interior. Hence, gel layers start to grow on the surface of each grain and those layers can expand more than that in SD-10 because the grain as a whole with its dry interior is not expanding. In other words, the increase in mesh size is constrained less by the pressure that expanding grains exert on each other. We suggest that this leads to a situation where the original pores are filled by a loose gel of a large mesh size while grain interiors, when starting to hydrate, form a denser gel with smaller mesh size. Ultimately, there will be a homogeneous hydration level throughout the tablet, but that process may take long time compared to the time scales explored here. In other words, inhomogeneous hydration creates a situation where diffusion through individual grains is slow which leads to a relatively slow release of the drug from the grains. However, once the dissolved drug is out in the original pore volume, filled with a gel of larger mesh size, a much faster displacement is obtained. Since the two length scales involved are disparate (path length for diffusion in the grains is an order of magnitude below the path length for diffusion through the tablet), the overall rate of drug transport will be high. We propose that this leads to the higher release rate observed from the RO-200 tablets. This suggestion is in line with that in a study by Gao et. al. [36], where the swelling of HPMC/lactose matrices was investigated by methods that provide information similar to that here, though in less detail. Based on the data in [36], inhomogeneous swelling was proposed as being responsible for a higher apparent drug diffusivity and release rate.

5. Conclusions

Solid dispersions can be prepared by different procedures yielding powders and, ultimately, tablets that exhibit different structures. Importantly, structural differences can lead to different release kinetics. We investigate here the mechanisms that lead to these latter differences by studying a model system with small direct effect of the drug properties on the release. To our aid, we have NMR imaging and NMR spectroscopy and scanning electron microscopy. Our advantage, when compared to most previous investigations, is to exploit the isotope and chemical selectivity available in NMR to record separately the release of the drug and the changes of water and polymer matrix properties as tablet hydration proceeds. Additionally, one-dimensional quantitative water distribution profiles are supported by two-dimensional cross-sectional images of the tablet, not quantitative but highly illustrative of the larger-scale structures which arise.

We compare tablets made from HPMC-based powders manufactured by two commonly used methods for solid dispersions: rotoevaporation/milling and spray drying. While these methods provide different grain types, too, we find that the effects we see arise as a consequence of the different grain size these methods provide. Air enclosed in the tablets seems to affect water ingress without any significant influence on polymer mobilization and drug release rates. This observation leads to the conclusion that water uptake by the originally dry polymer grains, rather than access to water nearby, seems to be the rate-limiting factor for swelling and release of drugs from the grains.

The information from all different experiments is amalgamated into a rather detailed and, at the same time, complex and partly unexpected picture. This contributes to a fundamental understanding of the dynamical processes that arise in reaction to bulk structural properties in two-component systems commonly applied in the solid dispersion concepts. We conclude that tablets that were prepared by rotoevaporation/milling and, therefore, contain larger particles, evolve into a more inhomogeneous gel than the gels that appear in spray-dried tablets with a smaller dry grain size. The primary reason for this is that larger grains hydrate less evenly which is a consequence of scaling laws for diffusion. We also find that, in rotoevaporated tablets, some water penetrates very quickly into the depth of the tablet, possibly through some large pores. Inhomogeneous gels with channels of large mesh size are proposed to allow faster drug diffusion through the gel and, consequently, a faster release into the aqueous phase.

Further investigations into the same topic could involve imaging of the time-dependent distribution of the drug substance,

accessible by some chemical shift-based NMR imaging methods or by incorporating drug substances with other NMR active nuclei (such as ^{19}F). Varying the molecular size of the drug substances involved could be useful to test the importance of mesh size; recall that diffusion depends in a strongly non-linear manner on the drug-mesh size ratio [34,35]. Testing more hydrophobic drug substances is also highly desirable. The latter direction, where drug particle release by tablet erosion is more significant [37], may call for approaches such as erosion chambers built into NMR probes [38]. In another direction, the effect of storage and storage conditions would potentially be useful to investigate.

Acknowledgements

We thank Pavel Yushmanov for manufacturing the sample holder which has been used in all experiments. This work has been supported by Novartis Pharma AG, the Swedish Research Council VR and Knut and Alice Wallenberg foundation.

References

[1] T. Vasconcelos, B. Sarmento, P. Costa, Solid dispersions as strategy to improve oral bioavailability of poor water soluble drugs, Drug Disc. Today 12 (2007) 1068–1075.
[2] D.A. Alderman, A review of cellulose ethers in hydrophilic matrices for oral controlled-release dosage forms, Int. J. Pharm. Technol. Prod. Manuf. 5 (1984) 1–9.
[3] M.E. Campos-Aldrete, L. Villafuerte-Robles, Influence of the viscosity grade and the particle size of HPMC on metronidazole release from matrix tablets, Eur. J. Pharm. Biopharm. 43 (1997) 173–178.
[4] A. Miranda, M. Millan, I. Caraballo, Investigation of the influence of particle size on the excipient percolation threshold of HPMC hydrophilic matrix tablets, J. Pharm. Sci. 96 (2007) 2746–2756.
[5] A.T.M. Serajuddin, Solid dispersion of poorly water-soluble drugs: early promises, subsequent problems, and recent breakthroughs, J. Pharm. Sci. 88 (1999) 1058–1066.
[6] K. Mitchell, J.L. Ford, D.J. Armstrong, P.N.C. Elliott, J.E. Hogan, C. Rostron, The influence of the particle size of hydroxypropylmethylcellulose K15M on its hydration and performance in matrix tablets, Int. J. Pharm. 100 (1993) 175–179.
[7] M.A. Dabbagh, J.L. Ford, M.H. Rubinstein, J.E. Hogan, Effects of polymer particle size, compaction pressure and hydrophilic polymers on drug release from matrices containing ethylcellulose, Int. J. Pharm. 140 (1996) 85–95.
[8] P.W.S. Heng, L.W. Chan, M.G. Easterbrook, X.M. Li, Investigation of the influence of mean HPMC particle size and number of polymer particles on the release of aspirin from swellable hydrophilic matrix tablets, J. Control. Release 76 (2001) 39–49.
[9] M.V. Velasco, J.L. Ford, P. Rowe, A.R. Rajabi-Siahboomi, Influence of drug: hydroxypropylmethylcellulose ratio, drug and polymer particle size and compression force on the release of diclofenac sodium from HPMC tablets, J. Control. Release 57 (1999) 75–85.
[10] S. Zuleger, B.C. Lippold, Polymer particle erosion controlling drug release. I. Factors influencing drug release and characterization of the release mechanism, Int. J. Pharm. 217 (2001) 139–152.
[11] R.W. Korsmeyer, R. Gurny, E. Doelker, P. Buri, N.A. Peppas, Mechanisms of Kcl release from compressed, hydrophilic, polymeric matrices – effect of entrapped air, J. Pharm. Sci. 72 (1983) 1189–1191.
[12] H. Hashim, A. Li Wan Po, Improving the release characteristics of water-soluble drugs from hydrophilic sustained release matrices by in situ gas generation, Int. J. Pharm. 35 (1987) 201–209.
[13] E. Karakosta, P.M. Jenneson, R.P. Sear, P.J. McDonald, Observations of coarsening of air voids in a polymer – highly-soluble crystalline matrix during dissolution, Phys. Rev. E 74 (2006) 011504.
[14] J.C. Richardson, R.W. Bowtell, K. Mader, C.D. Melia, Pharmaceutical applications of magnetic resonance imaging (MRI), Adv. Drug Delivery Rev. 57 (2005) 1191–1209.
[15] C.D. Melia, A.R. Rajabi-Siahboomi, R.W. Bowtell, Magnetic resonance imaging of controlled release pharmaceutical dosage forms, Pharm. Sci. Technol. Today 1 (1998) 32–39.
[16] J. Tritt-Goc, N. Pislewski, Magnetic resonance imaging study of the swelling kinetics of hydroxypropylmethylcellulose (HPMC) in water, J. Control. Release 80 (2002) 79–86.
[17] S. Harding, H. Baumann, T. Gren, A. Seo, NMR microscopy of the uptake, distribution and mobility of dissolution media in small, sub-millimetre drug delivery systems, J. Control. Release 66 (2000) 81–99.
[18] B.J. Fahie, A. Nangia, S.K. Chopra, C.A. Fyfe, H. Grondey, A. Blazek, Use of NMR imaging in the optimization of a compression-coated regulated release system, J. Control. Release 51 (1998) 179–184.
[19] A.R. Rajabi-Siahboomi, R.W. Bowtell, P. Mansfield, A. Henderson, M.C. Davies, C.D. Melia, Structure and behaviour in hydrophilic matrix sustained release dosage forms: 2. NMR-imaging studies of dimensional changes in the gel layer and core of HPMC tablets undergoing hydration, J. Control. Release 31 (1994) 121–128.
[20] C.A. Fyfe, A.I. Blazek, Investigation of hydrogel formation from hydroxypropylmethylcellulose (HPMC) by NMR spectroscopy and NMR imaging techniques, Macromolecules 30 (1997) 6230–6237.
[21] J. Tritt-Goc, J. Kowalczuk, Spatially resolved solvent interaction with glassy HPMC polymers studied by magnetic resonance microscopy, Solid State Nucl. Magn. Reson. 28 (2005) 250–257.
[22] J. Kowalczuk, J. Tritt-Goc, N. Pislewski, The swelling properties of hydroxypropyl methyl cellulose loaded with tetracycline hydrochloride: magnetic resonance imaging study, Solid State Nucl. Magn. Reson. 25 (2004) 35–41.
[23] A. Haase, J. Frahm, D. Matthaei, W. Hanicke, K.D. Merboldt, FLASH imaging, rapid NMR imaging using low flip-angle pulses, J. Magn. Reson. (1969) 67 (1986) 258.
[24] S. Gravina, D.G. Cory, Sensitivity and resolution of constant-time imaging, J. Magn. Reson. B 104 (1994) 53–61.
[25] S. Emid, J.H.N. Creyghton, High resolution NMR imaging in solids, Physica B+C 128 (1985) 81–83.
[26] P.T. Callaghan, Principles of Nuclear Magnetic Resonance Microscopy, Oxford University Press, New York, 1991.
[27] C. Dahlberg, A. Fureby, M. Schuleit, S.V. Dvinskikh, I. Furó, Polymer mobilization and drug release during tablet swelling. A ^{1}H NMR and NMR microimaging study, J. Control. Release 122 (2007) 199–205.
[28] C. Dahlberg, A. Millqvist-Fureby, M. Schuleit, Surface composition and contact angle relationships for differently prepared solid dispersions, Eur. J. Pharm. Biopharm. 70 (2008) 478–485.
[29] Dow Chemical Company, METHOCEL Cellulose Ethers, Technical handbook, in: Form No. 192-01062-0902, 2002.
[30] C.D. Melia, A.R. Rajabi-Siahboomi, A.C. Hodsdon, J. Adler, J.R. Mitchell, Structure and behaviour of hydrophilic matrix sustained release dosage forms: 1. The origin and mechanism of formation of gas bubbles in the hydrated surface layer, Int. J. Pharm. 100 (1993) 263–269.
[31] C.A. Fyfe, A.I. Blazek, Complications in investigations of the swelling of hydrogel matrices due to the presence of trapped gas, J. Control. Release 52 (1998) 221–225.
[32] R. Bowtell, J.C. Sharp, A. Peters, P. Mansfield, A.R. Rajabi-Siahboomi, M.C. Davies, C.D. Melia, NMR microscopy of hydrating hydrophilic matrix pharmaceutical tablets, Magn. Reson. Imag. 12 (1994) 361–364.
[33] J.L. Salomon, E. Doelker, P. Buri, Importance of technology and formulation for release mechanism of potassium-chloride contained in hydrophilic matrix. 1. Effect of viscosity and gelling percentage, Pharm. Acta Helv. 54 (1979) 82–85.
[34] L. Masaro, X.X. Zhu, Physical models of diffusion for polymer solutions, gels and solids, Prog. Polym. Sci. 24 (1999) 731–775.
[35] B. Amsden, Solute diffusion within hydrogels. Mechanisms and models, Macromolecules 31 (1998) 8382–8395.
[36] P. Gao, J.W. Skoug, P.R. Nixon, R. Ju, N.L. Stemm, I.K.-C. Sung, Swelling of hydroxypropyl methylcellulose matrix tablets. 2. Mechanistic study of the influence of formulation variables on matrix performance and drug release, J. Pharm. Sci. 85 (1996) 732–740.
[37] J.L. Ford, M.H. Rubinstein, F. McCaul, J.E. Hogan, P.J. Edgar, Importance of drug type, tablet shape and added diluents on drug release kinetics from hydroxypropylmethylcellulose matrix tablets, Int. J. Pharm. 40 (1987) 223–234.
[38] S. Abrahmsen-Alami, A. Körner, I. Nilsson, A. Larsson, New release cell for NMR microimaging of tablets: swelling and erosion of poly(ethylene oxide), Int. J. Pharm. 342 (2007) 105–114.